Magnetic Properties in Transition-Metal-Doped Gold Clusters: $M@Au_6$ (M = Ti, V, Cr)

Xi Li, Boggavarapu Kiran, Li-Feng Cui, and Lai-Sheng Wang*

Department of Physics, Washington State University, 2710 University Drive, Richland, Washington 99352, USA and W. R. Wiley Environmental Molecular Sciences Laboratory and Chemical Sciences Division, Pacific Northwest National Laboratory, Mississippi K8-88, Post Office Box 999, Richland, Washington 99352, USA

(Received 18 July 2005; published 16 December 2005)

The electronic structure and magnetic properties in a series of transition-metal-doped Au clusters, MAu_6^- (M = Ti, V, Cr), are investigated experimentally using photoelectron spectroscopy (PES) and density functional calculations. PES features due to the impurity atoms and the Au_6 host are clearly observed. It is found that all the MAu_6^- and MAu_6 clusters possess a planar structure, in which the transition metal atom is located in the center of an Au_6 ring and carries large magnetic moments (2, 3, and 4 μ_B for MAu_6, M = Ti, V, and Cr, respectively).

DOI: 10.1103/PhysRevLett.95.253401 PACS numbers: 36.40.Mr, 33.60.Cv, 73.22.−f

Although transition metal atoms with a partially filled d shell are magnetic, their magnetism is quenched or significantly reduced in the bulk due to chemical bonding that gives rise to crystal cohesion. For transition metal impurities in a nonmagnetic host, the hybridization of the impurity d states with the host metal plays a crucial role in determining the local magnetic moments, which is sensitive to both the local structure and the electronic nature of the host [1–4]. Atomic clusters provide a unique medium to explore magnetism because the cluster size, local structure, and atomic compositions can be readily controlled and varied [5–11]. Generally, the reduced coordination number and higher symmetry in clusters lead to narrower electronic bands and enhanced magnetization [5–9]. Gold clusters have been of considerable current interest in nanoscience because of the unique catalytic, electronic, and optical properties exhibited by small gold nanoparticles [12–18]. Transition-metal-doped gold clusters have also been actively pursued to tailor the desired structural, electronic, magnetic, and chemical properties for potential applications [19–27]. Here we report the generation of a series of transition-metal-doped gold clusters, MAu_6^- (M = Ti, V, Cr), which are investigated experimentally by photoelectron spectroscopy (PES) and theoretically using density functional theory (DFT). It is found that the magnetic moments of the impurity transition metal atoms are not quenched by the nonmagnetic gold host in the MAu_6 clusters, which possess total magnetic moments corresponding to the number of d electrons (2, 3, and 4 for M = Ti, V, Cr, respectively) localized in atomiclike unhybridized 3d orbitals of the dopands.

The experiment was performed using a laser vaporization magnetic-bottle PES apparatus [28]. The bimetallic MAu_6^- cluster anions were produced by laser vaporization of an Au/M (M = Ti, V, Cr) disk target and mass-separated using time-of-flight mass spectrometry. Photoelectron spectra of MAu_6^- were measured using a magnetic-bottle time-of-flight PES analyzer at three different photon energies: 355 (3.496 eV), 266 (4.661 eV), and 193 nm (6.424 eV) with an electron kinetic energy resolution of $\Delta E_k/E_k \sim 2.5\%$ (~25 meV for 1 eV electrons). The spectrometer was calibrated with the known spectrum of Au^- and Rh^-. Figure 1 shows the photoelectron spectra of MAu_6^- (M = Ti, V, Cr) at 193 nm with numerous well-resolved features. The spectra for all three species are very similar and all have very nearly identical electron binding energies. The spectra can be divided into two spectral regions (Fig. 1): region I in the low binding energy side between 3–4.5 eV and region II between 4.5 and 6.4 eV in the high binding energy side. Region I displays the only differences among the three species: more transitions are observed from M = Ti → V → Cr. Remarkably, region II is almost identical in all three spectra. These observations suggest that the spectral features in region I are from detachment of dopand-dominated orbitals, whereas region II is from the Au_6 motif of the bimetallic clusters. We note that spectral features in region II bear some amazing similarities to the valence-band part of the neat Au_6^- photoelectron spectrum [16]. The similarity of the photoelectron spectra of the three MAu_6^- species implies that these bimetallic clusters must have similar geometrical structures. The observation of the clear separation between spectral features of the dopand and the Au_6 motif in the MAu_6^- bimetallic clusters is unprecedented, suggesting a guest-host relationship between M and Au_6 and a special chemical interaction between the dopand and the host.

More fine features were resolved in the lower photon energy spectra (not shown) and allowed the adiabatic and vertical detachment energies of the ground state transition (X) to be accurately determined (Table I) [29]. The inset of Fig. 1(a) displays the 355 nm spectrum of $TiAu_6^-$, which was vibrationally resolved with a frequency of 160 ± 20 cm^{-1}. The observation of a single short vibrational progression suggested that there is very little geometrical change between the ground states of $TiAu_6^-$ and $TiAu_6$ and that they both have very high symmetry. We performed quantum calculations to identify the most stable structures of MAu_6^- and MAu_6 and to obtain insight into the nature of bonding between the transition metal guest and the nonmagnetic host [30]. An extensive structural search

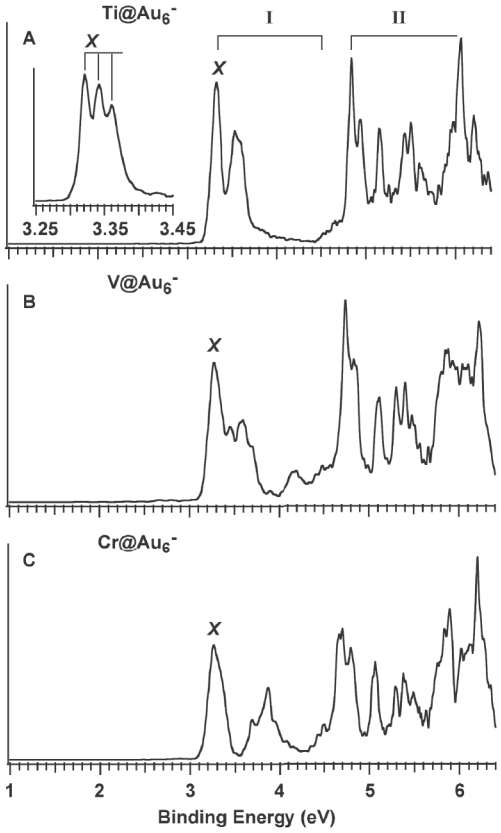

FIG. 1. Photoelectron spectra of MAu_6^- (M = Ti, V, and Cr) at 193 nm, (a) $TiAu_6^-$, (b) VAu_6^-, and (c) $CrAu_6^-$. The inset in Fig. 1(a) displays the 355 nm spectrum with a well-resolved vibrational progression for $TiAu_6$. The observed electronic transitions are labeled as two regions I and II: region I denotes photodetachment transitions mainly from the 3d-derived orbitals of the dopant atom and II denotes detachment transitions from gold 5d-derived orbitals (see text).

was performed. Among the numerous possible structural isomers two types of structures are important. First, since small gold clusters have been shown to be planar [15,16], we considered various two-dimensional (2D) structures. Second, we considered three-dimensional (3D) structures with six Au atoms surrounding a central impurity atom analogous to the icosahedral $W@Au_{12}$ cluster [19,20]. Many isomers were found and two structures, representing the two structural types, are given in Fig. 2.

TABLE I. Experimental adiabatic (ADE) and vertical (VDE) detachment energies of MAu_6^- (M = Ti, V, and Cr) compared to those calculated for the lowest energy isomers. All energies are in eV.

	Experimental		Theoretical	
	ADE	VDE	ADE	VDE
$TiAu_6^-$	3.32 ± 0.02	3.32 ± 0.02	3.28	3.29
VAu_6^-	3.23 ± 0.02	3.25 ± 0.02	3.20	3.23
$CrAu_6^-$	3.23 ± 0.02	3.25 ± 0.02	3.20	3.23

The most stable structure for MAu_6^- and MAu_6 (M = Ti, V, and Cr), is a 2D structure with the transition metal atom sitting in the center of an Au_6 ring [Fig. 2(a)]. Other lower-symmetry 2D structures are all much higher in energy for all three clusters. The high symmetry 3D octahedral arrangement is not a stable structure and geometry optimization led to a distorted isomer [Fig. 2(b)], which is much higher in energy than the 2D ring structure. The Au-M distance in the 2D MAu_6^- cluster is relatively constant for all the three central atoms and averages about 2.69 Å, which is longer than the normal Au-M distance, for example, the Au-Ti distance in tetrahedral $TiAu_4$ is 2.42 Å [31]. A recent DFT study on MAu_n^+ cations showed a similar ring structure to be the ground state for VAu_6^+ and low-lying isomers for $TiAu_6^+$ and $CrAu_6^+$ [27]. The ground state of $TiAu_6^+$ was shown to be a lower-symmetry 2D structure while that of $CrAu_6^+$ was shown to be a 3D structure. The Au-M distance in the ring structure of the MAu_6^+ cations is in the range of 2.73 to 2.76 Å, slightly longer than the M-Au distance in the MAu_6^- anions.

It should be noted that all the ground state 2D structures of MAu_6^- have high spins, whereas the 3D structures tend to have low spins (Fig. 2). The doublet $TiAu_6^-$ and quartet $CrAu_6^-$ form perfectly symmetrical D_{6h} structures. However, due to the Jahn-Teller effect, the triplet VAu_6^- has a very slight in-plane distortion to a lower-symmetry D_{2h} structure with very minor bond length changes. Although the most stable isomer for neutral MAu_6 is also the Au_6 ring with the dopant at the center, for $TiAu_6$ the 2D structure is only more stable than the 3D one by 0.15 eV. However, for VAu_6 and $CrAu_6$ the 2D structure is overwhelmingly favored (0.75 and 2.72 eV in favor of the 2D structure for VAu_6 and $CrAu_6$, respectively). The neutral ground state structures all have marginally distorted geometries from the perfect D_{6h} molecular wheels. Because of the very flat potential energy surfaces, these distortions have negligible effect on the energies from the corresponding planar forms, consistent with the sharp ground state PES transitions. We found that all the neutral MAu_6 ring structures prefer higher spin multiplicities (S = 3, 4, and 5

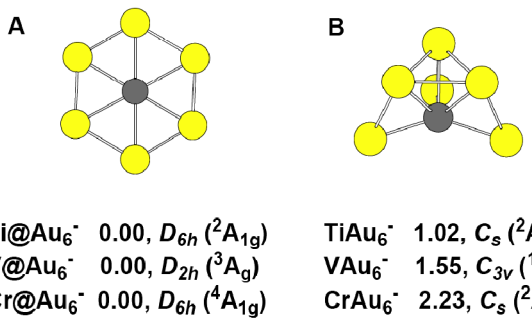

FIG. 2 (color online). Optimized structures for MAu_6^- (M = Ti, V, and Cr) using density functional theory at the PW91-SDD level. Relative energies are given in eV. (a) The most stable isomer; (b) The second isomer.

for M = Ti, V, and Cr, respectively) compared to the corresponding anions. We note that the ring structures of the MAu_6^+ cations were also predicted to have high spins ($S = 4$, 5, and 6 for M = Ti, V, and Cr, respectively) [27].

To validate the theoretical predictions, we computed the adiabatic and vertical detachment energies, as compared with the experimental values in Table I. All the computed detachment energies agree very well with the experimental results. The calculated vibration frequency for the totally symmetric mode for the ground state of $TiAu_6$ is 137 cm^{-1}, which also compares well to the observed value (160 ± 20 cm^{-1}). The closeness of the calculated adiabatic and vertical detachment energies for each species is consistent with the negligible geometry change between the anion and neutral ground state structures. The excellent agreement between the experimental and theoretical results lend considerable credence to the obtained planar wheel structures for MAu_6^- and MAu_6 and their high spin multiplicities.

Figure 3 displays a schematic molecular orbital correlation diagram for the three 2D MAu_6^- clusters and their valence orbital pictures, which provide insight into the observed spectral features and the nature of bonding between the dopand and the Au_6 ring. The energy levels for all the clusters separate into two distinct regions with a considerable energy gap. The frontier orbitals consist of almost pure d orbitals from the central dopant, whereas all the occupied levels derived from the Au_6 ring lie significantly deeper. These orbital level schemes are consistent with the photoelectron spectra (Fig. 1). The bonding interactions between the dopant and the Au_6 ring come by symmetry from the overlaps between the in-plane d_{xy} and $d_{x^2-y^2}$ orbitals with the antibonding 6s orbitals of the Au_6 ring. The first detachment channel, common for all three MAu_6^- clusters, is the removal of the d_{xy} β electron.

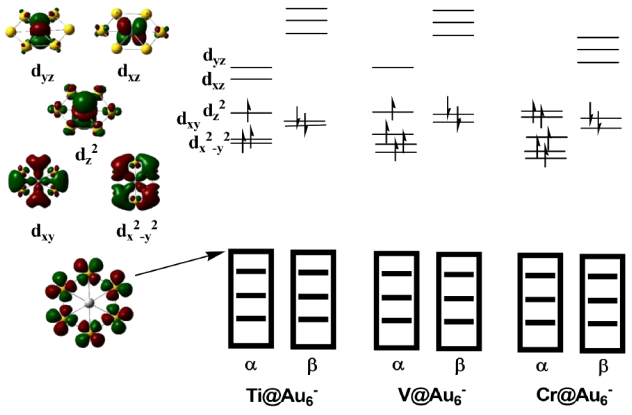

FIG. 3 (color online). Molecular orbitals (MOs) and MO energy level correlation diagram for $M@Au_6^-$ (M = Ti, V, and Cr). The mainly M 3d orbitals (top) are well separated from the Au-derived orbitals represented by boxes. Pictures for the five M d orbitals and one of the topmost Au-derived orbitals are shown (left).

This explains why the first ADE's for all three MAu_6^- clusters are remarkably similar and also explains the observation of the single vibrational progression in the 355 nm spectrum of $TiAu_6^-$ (Fig. 1) due to the ring breathing mode. As the dopant changes from Ti to Cr, the extra d electrons fill the nonbonding, atomiclike d orbitals, whose binding energies gradually increase. As a result extra detachment bands appear to fill the gap between the two main regions in the photoelectron spectra of VAu_6^- and $CrAu_6^-$ (Fig. 1).

Thus the bonding in the MAu_6^- bimetallic clusters can be viewed as an Au_6 ring interacting with an M^-, which possesses a d^5, d^6, and d^7 valence configuration for M = Ti, V, and Cr, respectively, (i.e., the 4s electrons are promoted to the 3d orbitals). Four of these electrons (two α and two β) are involved in the bonding between M^- and Au_6, leaving 1, 2, and 3 unpaired spins in the MAu_6^- anions for M = Ti, V, and Cr, respectively. In the neutral clusters, one of the bonding electrons ($d_{xy}\beta$) is detached, resulting in 2, 3, and 4 unpaired spins in MAu_6 for M = Ti, V, and Cr, respectively. These unpaired spins occupy atomiclike d orbitals and the number of spins correspond exactly to the number of unpaired d electrons in the atoms (except for Cr, which has a d^5s^1 ground state configuration). Thus the MAu_6 bimetallic clusters possess atomiclike magnetism, carrying magnetic moments of 2, 3, and 4 μ_B for M = Ti, V, and Cr, respectively. Although there is considerable chemical bonding between the impurity atom and the Au_6 ring, the atomic magnetism is maintained in the bimetallic clusters. The Au_6 ring acts as a host protecting the spins of the central dopant atoms, whereas the dopant atom helps stabilize the Au_6 ring structure because the bare Au_6 cluster is known to have a D_{3h} triangular structure [15,16]. Thus the transition metal dopant atom and the Au_6 ring have a unique host-guest interaction, stabilizing the ring structure and giving rise to the atomic magnetism.

It is well-known that the local magnetic properties of an impurity transition metal atom strongly depend on the local environment. The planar structure of the MAu_6 clusters is important for their atomiclike magnetism because in the planar geometry only the two in-plane d orbitals (d_{xy} and $d_{x^2-y^2}$) can interact with the substrate by symmetry while the three out-of-plane d orbitals (d_{xy}, d_{yz}, and d_{z^2}) have little interaction with the substrate and behave atomiclike. In 3D structures, all five d orbitals may interact with the substrate; and depending on the strength of this interaction the magnetic moment of the impurity atom may be completely quenched. For example, a Cr atom inside an Au_{12} cage has been shown to exhibit no magnetic moment [26]. We note the ring-shaped MAu_6^+ cations [27] have all been shown to exhibit large magnetic moments ($S = 4, 5, 6$ for M = Ti, V, Cr, respectively) even higher than the neutral MAu_6 clusters, corresponding to the removal of both minority spins in the d orbital manifold (Fig. 3). However, these minority spins in the d_{xy} and $d_{x^2-y^2}$ orbitals are also

responsible for the M and Au_6 ring bonding interactions. Thus, the removal of these electrons weakens the stability of the planar ring structures in the MAu_6^+ cations, making other structures energetically competitive or even more favored for the MAu_6^+ cations [27].

Preliminary theoretical and experimental results show that all transition metal atoms with open d shells can stabilize the Au_6 ring structure. In other words, the Au_6 ring in the MAu_6 system serves as a perfect, maybe the smallest, host to store a single transition metal atom, analogous to endohedral fullerenes ($M@C_{60}$, $M =$ alkali metal, alkali earth, rare earth, and rare gas atoms), although no transition metal atoms can be stored inside the fullerenes [32,33]. We performed preliminary DFT calculations in which $Ti@Au_6$ clusters are laid on a nonmagnetic surface such as a graphite surface, and found that the atomiclike magnetic moments in $Ti@Au_6$ are not quenched by the surface. Thus the $M@Au_6$ guest-host bimetallic clusters may serve as an ideal system to investigate impurity atoms in planar geometries. Continued experimental and theoretical studies of similar impurity doped clusters may lead to the discovery of new families of molecular magnets with tunable magnetic properties.

The experimental work was supported by the NSF (CHE-0349426) and the John Simon Guggenheim Foundation and performed at the EMSL, a national scientific user facility sponsored by the U.S. DOE's Office of Biological and Environmental Research and located at PNNL, operated for DOE by Battelle.

*To whom correspondence should be addressed.
E-mail: ls.wang@pnl.gov

[1] J. B. Staunton, Rep. Prog. Phys. **57**, 1289 (1994).
[2] D. Bagayoko, P. Blaha, and J. Callaway, Phys. Rev. B **34**, 3572 (1986).
[3] D. Guenzburger and D. E. Ellis, Phys. Rev. Lett. **67**, 3832 (1991).
[4] N. Papanikolaou, N. Stefanou, R. Zeller, and P. H. Dederichs, Phys. Rev. Lett. **71**, 629 (1993).
[5] F. Liu, S. N. Khanna, and P. Jena, Phys. Rev. B **43**, 8179 (1991).
[6] I. M. L. Billas, A. Chatelain, and W. A. de Heer, Science **265**, 1682 (1994).
[7] S. E. Apsel, J. W. Emmert, J. Deng, and L. A. Bloomfield, Phys. Rev. Lett. **76**, 1441 (1996).
[8] G. M. Pastor, R. Hirsch, and B. Muhlschlegel, Phys. Rev. Lett. **72**, 3879 (1994).
[9] M. B. Knickelbein, Phys. Rev. Lett. **86**, 5255 (2001).
[10] Q. Sun, X. G. Gong, Q. Q. Zheng, D. Y. Sun, and G. H. Wang, Phys. Rev. B **54**, 10 896 (1996).
[11] Q. Sun, Q. Wang, J. Z. Yu, Z. Q. Li, J. T. Wang, and Y. Kawazoe, J. Phys. I **7**, 1233 (1997).
[12] M. Haruta, Catal Today **36**, 153 (1997).
[13] P. Schwerdtfeger, Angew. Chem., Int. Ed. **42**, 1892 (2003).
[14] H. Häkkinen, M. Moseler, and U. Landman, Phys. Rev. Lett. **89**, 033401 (2002).
[15] F. Furche, R. Ahlrichs, P. Weis, C. Jacob, S. Gilb, T. Bierweiler, and M. Kappes, J. Chem. Phys. **117**, 6982 (2002).
[16] H. Häkkinen, B. Yoon, U. Landman, X. Li, H. J. Zhai, and L. S. Wang, J. Phys. Chem. A **107**, 6168 (2003).
[17] J. Li, X. Li, H. J. Zhai, and L. S. Wang, Science **299**, 864 (2003).
[18] M. S. Chen and D. W. Goodman, Science **306**, 252 (2004).
[19] P. Pyykkö and N. Runeberg, Angew. Chem., Int. Ed. **41**, 2174 (2002).
[20] X. Li, B. Kiran, J. Li, H. J. Zhai, and L. S. Wang, Angew. Chem., Int. Ed. **41**, 4786 (2002).
[21] K. Koyasu, M. Mitsui, A. Nakajima, and K. Kaya, Chem. Phys. Lett. **358**, 224 (2002).
[22] H. Häkkinen, S. Abbet, A. Sanchez, U. Heiz, and U. Landman, Angew. Chem., Int. Ed. **42**, 1297 (2003).
[23] H. Tanaka, S. Neukermans, E. Janssens, R. E. Silverans, and P. Lievens, J. Am. Chem. Soc. **125**, 2862 (2003).
[24] S. Neukermans, E. Janssens, H. Tanaka, R. E. Silverans, and P. Lievens, Phys. Rev. Lett. **90**, 033401 (2003).
[25] E. Janssens, H. Tanaka, S. Neukermans, R. E. Silverans, and P. Lievens, Phys. Rev. B **69**, 085402 (2004).
[26] S. Y. Wang, J. Z. Yu, H. Mizuseki, Q. Sun, C. Y. Wang, and Y. Kawazoe, Phys. Rev. B **70**, 165413 (2004).
[27] M. B. Torres, E. M. Fernandez, and L. C. Balbas, Phys. Rev. B **71**, 155412 (2005).
[28] L. S. Wang, H. S. Cheng, and J. Fan, J. Chem. Phys. **102**, 9480 (1995).
[29] The ADE and VDE for $TiAu_6^-$ were measured readily from the vibrationally resolved spectrum at 355 nm [see inset of Fig. 1(a)]. For VAu_6^- and $CrAu_6^-$, where vibrational fine structures were not clearly observed, their ADEs were measured from the 355 nm spectra by drawing a straight line along the leading edge of the threshold band and adding the instrumental resolution to the intersection with the binding energy axis. The VDEs were measured from the maximum of the threshold band.
[30] Geometry optimizations were carried with relativistic density functional theory at the generalized gradient approach level using Perdew-Wang exchange-correlation functionals [J. P. Perdew and Y. Wang, Phys. Rev. B **45**, 13 244 (1992)]. For all atoms energy adjusted Stuttgart effective core potentials were used in order to take into account relativistic effects [D. Andrae, U. Haussermann, M. Dolg, H. Stoll, and H. Preuss, Theor. Chim. Acta **77**, 123 (1990)]. The number of valance electrons for Ti is 12, 13 for V, 14 for Cr, and 19 for Au. The $6s5p3d$ valance basis set with one "f-type" polarization function was used for Ti, V, and Cr and two "f" functions (exponents 0.20, 1.19) were used for the Au atoms. The vertical detachment energies were calculated using delta-SCF procedures. All calculations were done with the GAUSSIAN 03 program. All the structures reported here have positive vibrational frequencies towards the nuclear displacements and therefore corresponds to the potential energy minima.
[31] L. Gagliardi, J. Am. Chem. Soc. **125**, 7504 (2003).
[32] L. S. Wang, J. M. Alford, Y. Chai, M. Diener, G. E. Scuseria, and R. E. Smalley, Chem. Phys. Lett. **207**, 354 (1993).
[33] M. Saunders, H. A. Jimenez-Vazquez, R. J. Cross, and R. J. Poreda, Science **259**, 1428 (1993).